Wave Height Estimation Methods for Non-Breaking Waves Using Video Images

Tochukwu Ngene[1], Tiago Abreu[2], Paulo A. Silva[3] and Paulo Baptista[4]

[1] CESAM & Department of Geosciences, University of Aveiro, Aveiro, Portugal
[2] CESAM & Civil Engineering Department, ISEP, Polytechnic of Porto, Porto, Portugal
[3] CESAM & Department of Physics, University of Aveiro, Aveiro, Portugal
[4] CESAM & Department of Geosciences, University of Aveiro, Aveiro, Portugal
ngene@ua.pt

Abstract.
Optical monitoring systems have become essential tools for measuring hydrodynamic parameters in the shoreface zone. They offer continuous data collection over large spatial areas, making them highly valuable in coastal research. However, accurately estimating wave heights from optical imagery remains a challenge due to the complexities of wave interactions, variations in camera configurations, and environmental conditions. This study evaluates two methodologies for estimating wave heights in the non-breaking zone using UAV footage, building on the limitations of previous techniques. The methods automatically detect waves using image processing techniques, initially measured in pixels. These pixel-based measurements are then converted to real-world coordinates (meters) through geometric transformations. A central focus was the variability of wave height estimates across different regions of interest (ROIs) of the image. The findings emphasize the critical role of optimal camera placement in enhancing measurement accuracy. This analysis contributes to advancing optical monitoring techniques, improving hydrodynamic parameter estimation, and better understanding dynamic coastal environments.

Keywords: Nearshore hydrodynamics, region of interest, video monitoring, wave height estimation.

1 Introduction

The derivation of wave heights from video imagery in the nearshore zone relies on the significant alteration in optical properties, as the imaging mechanism captures surface reflections [1]. Wave heights have been estimated by stereographic configurations in non-breaking zones [2][3], a method that is practically infeasible in open sea conditions. In breaking zones, time-stack images from a single camera have been employed [4], but this approach lacks consistency in the shoaling zone, where breaking waves and the characteristic white foam are absent.

Wave dynamics and environmental conditions, among other variables, are largely uncontrollable in natural settings and impact wave height measurements. In contrast,

camera configuration such as tilt, rotation, and height can be adjusted to align with the user's intent. Unmanned Aerial Vehicles (UAVs) offer a notable advantage in this context, allowing for the adjustment and optimization of all camera parameters on flight surveys over fixed cameras. Although geometric correction techniques aim to standardize measurements throughout the image, it is essential to assess the region of interest (ROI) where the results are most accurate and uniform.

This study evaluates how variations in ROI in an image affect the estimation of wave heights by comparing two methods.

2 Study Area and Video Settings

The study was conducted at Costa Nova Beach (Fig. 1), located in the Aveiro district on Portugal's western coast. Costa Nova is exposed to high-energy Atlantic waves, particularly during the winter, when wave heights can exceed 3-4 meters due to northwesterly swells. In summer, wave heights typically range between 0.5 and 2 meters. The video recording for the study was taken on November 17, 2023, starting at 16:15, under favorable weather conditions with 11% cloud cover and a wind speed of 5 km/h. The forecasted wave conditions are defined by a significant wave height (H_s) of 1.4 m, a wave period (T) of 9 seconds, and a direction (Dir) of west-southwest (WSW).

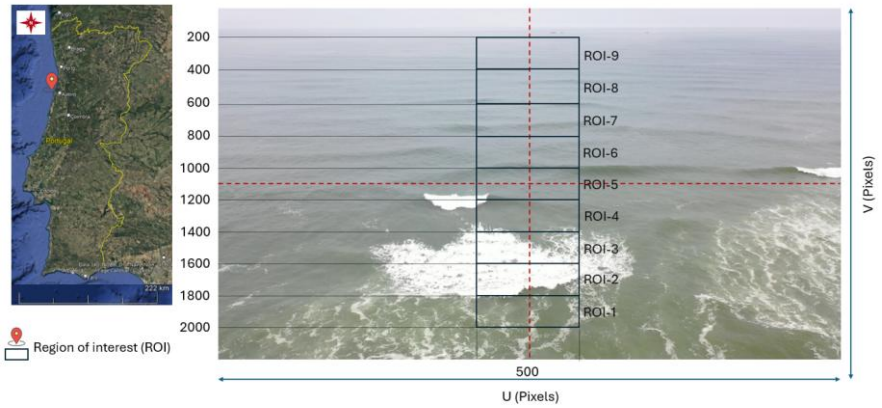

Fig. 1. (a) Study area and (b) segmented nine regions of interest (ROI) defined in the center of the image.

Aerial imaging for this study was conducted using the DJI Mavic 2 Pro, equipped with a Hasselblad L1D-20c camera featuring a 1-inch CMOS sensor. This sensor enhances light capture and significantly improves image quality, particularly in comparison to most commercial drones, enabling high-resolution imaging even in varied lighting conditions.

As this is the initial phase of developing a robust wave height estimation technique from images in the shoaling zone, a 2-minute video was recorded in 4K resolution (3840 × 2160 pixels) at 30 frames per second (*fps*), generating a total of 3,600 frames. This frame rate facilitated a detailed visual inspection of the extracted frames during

image processing and feature extraction, allowing for the evaluation of different segmentation techniques while minimizing computational costs.

The drone was operated at a consistent altitude of 49.8 meters above sea level, with the camera set at a tilt angle of 65 degrees. This configuration was chosen to optimize the field of view and enhance the capture of fine details necessary for the study.

3 Wave Heights Estimation Methods

Two methods were developed following the approach proposed by [4]. This analysis aimed to assess the variation in estimated wave heights (H_w) across different frames (with one frame extracted per second to minimize computational cost) and the corresponding significant wave heights (H_s) along the ROI in the time-series images. To analyze the variation of wave heights across the image, nine regions of interest (ROI-1 to ROI-9) were selected, each corresponding to 200 pixels heights and 500 pixels width as shown in Fig. 1b. This subdivision enables a detailed analysis of how wave heights vary across different areas, offering insights into spatial patterns and trends in the data. Image processing techniques, such as filtering and segmentation, were applied to each frame to extract the largest observed wave features (Fig. 2b), ROIs with undetected waves (Fig. 2a) were removed, followed by rectification using Eqs. (2) and (4).

(a) (b)

Fig. 2. (a) Undetected waves height in breaking zone, (b) Detected wave height (white features) in non-breaking zone.

After extracting the segmented wave features in pixels (H_i), Method 1 was applied by first determining the trough, crest, and still water level (*SWL*) of each wave using Eq. (1). The H_i was then converted to real-world units based on the image-camera geometry relationship established in Eq. (2) and shown in Fig. 3a [4]. K = 1/3 and H_c is the camera height.

$$SWL = z_{trough} + K\left(z_{crest} - z_{trough}\right), \tag{1}$$

$$H_w = \frac{H_c}{1-K} \times \left(\frac{(SWL-OA)-(z_{crest}-OA)}{SWL-OA}\right). \tag{2}$$

Method 2 relies on the effective focal length (*f*) at a specific zoom level, the vertical field of view (*FOV*), and the image height (*v*) of the ROI, which is determined using the derived geometry using Eq. (3). The ROI is designed to be appropriately sized to

capture an approximation of the largest feature H_i extracted in each frame, measured in pixels. The conversion from image coordinates to world coordinates is performed (Fig. 3b) using the calculated vertical ground sampling distance (*GSD*) in Eqs. (4) and (5). H_w was determined by multiplying H_i by *GSD*.

$$FOV = 2 \times tan^{-1}\left(\frac{Sensor\ height}{2 \times f}\right), \tag{3}$$

$$GSD = \frac{sample\ distance\ (m)}{image\ pixels\ (pixels)} = \frac{H_c - s}{v}, \tag{4}$$

$$s = tan\Theta_t \times H_c tan\emptyset_z = tan\Theta_t \times x, \tag{5}$$

where $\emptyset_z = 90 - \frac{FOV}{2} - \Theta_t,\ and\ \Theta_t = tilt\ angle.$

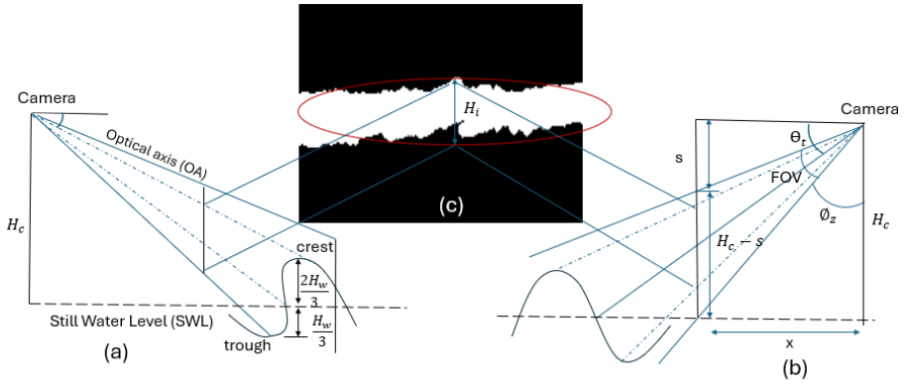

Fig. 3. (a) Geometric rectification of Method 1 (reproduced and modified from [4]), (b) Geometric rectification of Method 2, (c) Extracted wave height (H_i) in pixels.

Here, H_s was determined by calculating the average height of the highest one-third of the estimated waves of each image.

4 Results and Discussions

In this section, we present the analysis of wave features in the breaking zones, focusing on ROIs 6 to 9. Since the extracted features are based on the inverted segmented foreground, the surf foam influenced the accuracy of the measurements, highlighting the method's inefficiency in breaking zones as shown in Fig. 1a. Hence, ROIs 1 to 5 were excluded from further analysis.

Overall, the results show a strong agreement between both methodologies across the analyzed ROIs, with the curve shapes following a consistent pattern, as illustrated in Fig. (4). This indicates minimal variation in the estimated wave heights across the ROIs. ROIs 6 to 8 exhibit better alignment, with lower absolute differences in H_s as shown in

Table 1. Moreover, since these ROIs are located near the optical center of the image, where the influence of distortion is minimized, the methods achieve maximum accuracy at ROIs 6 and 7. The lower H_s values in ROI 8 may result from undetected features as the ROI moves farther from the image center. Additionally, ROI-9 shows some misalignment, which occurs because the number of detectable features decreases as the image height diminishes, likely due to the camera's position being nearly outside the field of view.

Table 1. Estimated significant wave heights and their respective absolute difference in the selected ROI.

ROI	Image height/position (pixels)	Significant wave height (m)		
		Method 1	Method 2	|Differences|
6	800:1000	0.93	1.07	0.15
7	600:800	0.93	1.06	0.13
8	400:600	0.55	0.56	0.01
9	200:400	1.47	1.70	0.23

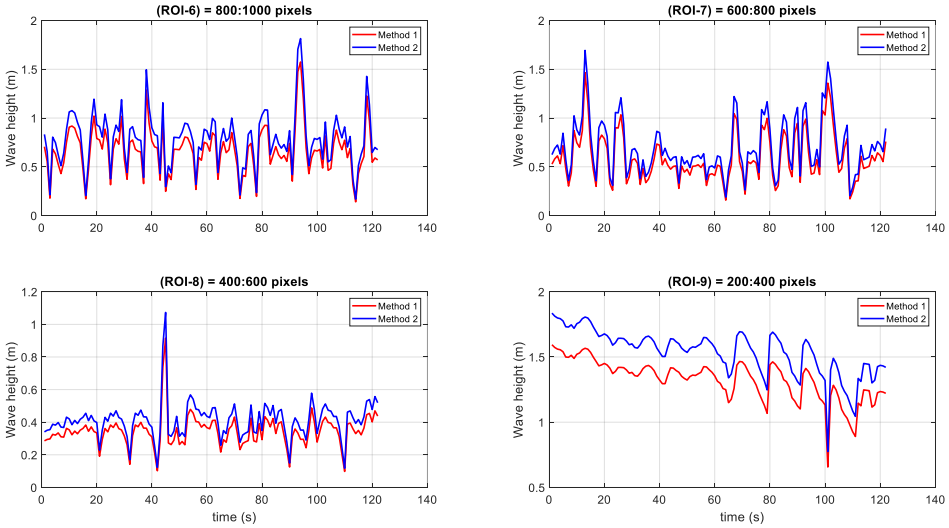

Fig. 4. Time series of the computed wave heights from method 1 (red) and 2 (blue) at the analyzed ROI, the x-axis represents the largest wave extracted from each frame at a rate of one frame per second.

5 Conclusion

Understanding the impact of camera orientation on feature detection enables practitioners to optimize their systems for more accurate wave parameter measurements. Ensuring the camera is oriented to clearly capture key objects is essential, as this reduces the need for costly re-installations of fixed cameras or repeated UAV surveys.

The methods outlined in this study show consistent results across all extracted ROI in the non-breaking zones. To achieve ideal accuracy, study areas should be centered within the image. While H_s values for methods 1 and 2 show slight variation across the ROI, further validation using additional hydrodynamic sensors is recommended to enhance the methods' reliability.

Acknowledgements

Thanks to FCT/MCTES for the financial support to CESAM, (UIDP/50017/2020+UIDB/50017/2020+LA/P/0094/2020), through national funds. Content produced within the scope of the Agenda “NEXUS - Pacto de Inovação – Transição Verde e Digital para Transportes, Logística e Mobilidade”, financed by the Portuguese Recovery and Resilience Plan (PRR), with no. C645112083-00000059 (investment project no. 53).

References

1. Almar, R., Cienfuegos, R., Catalán, P. A., Michallet, H., Castelle, B., Bonneton, P., & Marieu, V. A.: New breaking wave height direct estimator from video imagery. Coastal Engineering, 61(1), 42–48 (2012).
2. Andriolo, U., Mendes, D., & Taborda, R.: Breaking wave height estimation from timex images: Two methods for coastal video monitoring systems. Remote Sensing, 12(2), (2020).
3. Benetazzo, A.: Measurements of short water waves using stereo matched image sequences. Coastal Engineering, 53(12), 1013–1032 (2006).
4. Colvin, J., Lazarus, S., & Splitt, M.: Extracting nearshore wave properties from video: A new method for coastal estuaries. Estuarine, Coastal and Shelf Science, 246 (2020).
5. de Vries, S., Hill, D. F., de Schipper, M. A., & Stive, M. J. F.: Remote sensing of surf zone waves using stereo imaging. Coastal Engineering, 58(3), 239–250 (2011).